Evidence for *CP* Violation in $B^+ \to p\bar{p}K^+$ Decays

R. Aaij *et al.*[*]
(LHCb Collaboration)

(Received 22 July 2014; published 29 September 2014)

Three-body $B^+ \to p\bar{p}K^+$ and $B^+ \to p\bar{p}\pi^+$ decays are studied using a data sample corresponding to an integrated luminosity of 3.0 fb^{-1} collected by the LHCb experiment in proton-proton collisions at center-of-mass energies of 7 and 8 TeV. Evidence of *CP* violation in the $B^+ \to p\bar{p}K^+$ decay is found in regions of the phase space, representing the first measurement of this kind for a final state containing baryons. Measurements of the forward-backward asymmetry of the light meson in the $p\bar{p}$ rest frame yield $A_{\rm FB}(p\bar{p}K^+, m_{p\bar{p}} < 2.85\ {\rm GeV}/c^2) = 0.495 \pm 0.012\ ({\rm stat}) \pm 0.007\ ({\rm syst})$ and $A_{\rm FB}(p\bar{p}\pi^+, m_{p\bar{p}} < 2.85\ {\rm GeV}/c^2) = -0.409 \pm 0.033\ ({\rm stat}) \pm 0.006\ ({\rm syst})$. In addition, the branching fraction of the decay $B^+ \to \bar{\Lambda}(1520)p$ is measured to be $\mathcal{B}(B^+ \to \bar{\Lambda}(1520)p) = (3.15 \pm 0.48\ ({\rm stat}) \pm 0.07\ ({\rm syst}) \pm 0.26\ ({\rm BF})) \times 10^{-7}$, where BF denotes the uncertainty on secondary branching fractions.

DOI: 10.1103/PhysRevLett.113.141801 PACS numbers: 13.25.Hw, 11.30.Er

Direct *CP* violation can appear as a rate asymmetry in the decay of a particle and its *CP* conjugate, and it can be observed when at least two amplitudes, carrying different weak and strong phases, contribute to the final state. For B mesons, it was observed for the first time in two-body $B^0 \to K^+\pi^-$ decays [1,2]. The weak phases are sensitive to physics beyond the Standard Model that may appear at a high energy scale, and their extraction requires a determination of the relative strong phases. Three-body decays are an excellent laboratory for studying strong phases of interfering amplitudes. In particular, charmless decays of B^+ mesons $B^+ \to K^+\pi^-\pi^+$, $B^+ \to K^+K^-K^+$, $B^+ \to \pi^+\pi^-\pi^+$, and $B^+ \to K^+K^-\pi^+$ have been investigated recently [3–5]. (Throughout the Letter, the inclusion of charge conjugate processes is implied, except in the definition of *CP* asymmetries.) Similar studies have been conducted for the baryonic final states $B^+ \to p\bar{p}K^+$ and $B^+ \to p\bar{p}\pi^+$ [6]. In the $B^+ \to h^+h^-h^+$ decays ($h = \pi$ or K throughout this Letter), large asymmetries, not necessarily associated to resonances, have been observed in the low K^+K^- and $\pi^+\pi^-$ mass regions. These observations suggest that rescattering between $\pi^+\pi^-$ and K^+K^- pairs may play an important role in the generation of the strong phase difference needed for *CP* violation to occur [7]. The $B^+ \to p\bar{p}h^+$ decays, although sharing the same quark-level diagrams, may exhibit different behavior due to the baryonic nature of two out of the three final-state particles.

This Letter reports the first evidence for *CP* violation in charmless $B^+ \to p\bar{p}K^+$ decays. These decays are studied in the region with invariant mass $m_{p\bar{p}} < 2.85\ {\rm GeV}/c^2$, below the charmonium resonances threshold. In addition, a more accurate measurement of the branching fraction of the decay $B^+ \to \bar{\Lambda}(1520)p$ is performed, using the reconstruction of $\bar{\Lambda}(1520) \to K^+\bar{p}$ decays, and improved determinations of the spectra and angular asymmetries are also reported. The mode $B^+ \to J/\psi(\to p\bar{p})K^+$ serves as a control channel. The data used have been collected with the LHCb detector and correspond to 1.0 and 2.0 fb^{-1} of integrated luminosity at 7 and 8 TeV center-of-mass energies in pp collisions, respectively. The data samples are analyzed separately and the results are averaged.

The LHCb detector is a single-arm forward spectrometer covering the pseudorapidity range $2 < \eta < 5$, described in detail in Ref. [8]. The detector allows for the reconstruction of both charged and neutral particles. For this analysis, the ring-imaging Cherenkov detectors [9]—distinguishing pions, kaons, and protons—are particularly important.

The analysis uses simulated events generated by PYTHIA 8.1 [10] with a specific LHCb configuration [11]. Decays of hadronic particles are described by EVTGEN [12], in which final-state radiation is generated using PHOTOS [13]. The interaction of the generated particles with the detector and its response are implemented using the GEANT4 toolkit [14], as described in Ref. [15]. Nonresonant $B^+ \to p\bar{p}h^+$ events are simulated, uniformly distributed in phase space, to study the variation of efficiencies across the Dalitz [16] plane, as well as resonant modes such as $B^+ \to J/\psi(\to p\bar{p})K^+$, $B^+ \to \eta_c(\to p\bar{p})K^+$, $B^+ \to \psi(2S)(\to p\bar{p})K^+$, $B^+ \to \bar{\Lambda}(1520)(\to K^+\bar{p})p$, and $B^+ \to J/\psi(\to p\bar{p})\pi^+$.

Three charged particles are combined to form $B^+ \to p\bar{p}h^+$ decay candidates. The discrimination of signal from background is done through a multivariate analysis using a boosted decision tree (BDT) classifier [17]. Input quantities include kinematic and topological variables related to the B^+ candidates and the individual tracks. The momentum,

[*] Full author list given at the end of the article.

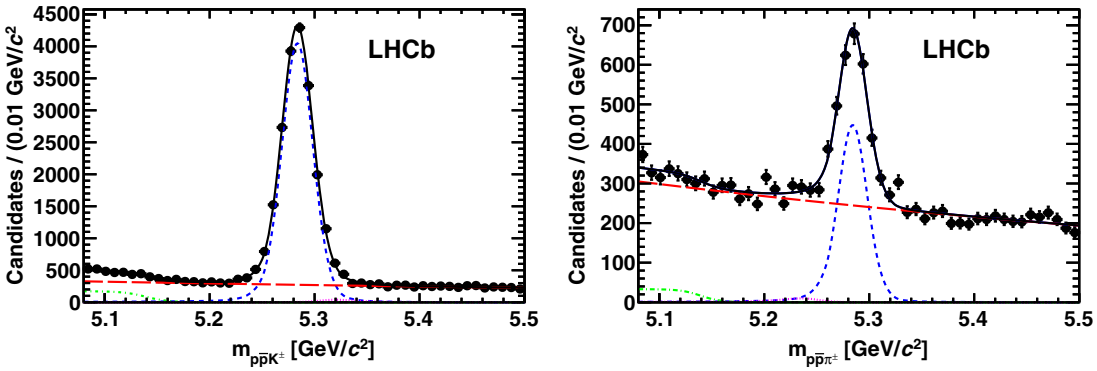

FIG. 1 (color online). Invariant mass distributions of $p\bar{p}K^+$ (left panel) and $p\bar{p}\pi^+$ (right panel) candidates. The points with error bars represent data. The solid black line represents the total fit function. The components are represented by blue dashed (signal), purple dotted (cross feed), red long-dashed (combinatorial background), and green dash-dotted (partially reconstructed background) curves.

vertex, and flight distance of the B^+ candidate are exploited, and track fit quality criteria, impact parameter, and momentum information of final-state particles are also used. The BDT is trained using simulated signal events and events in the high sideband of the $p\bar{p}h^+$ invariant mass $(5.4 < m(p\bar{p}h^+) < 5.5\ \mathrm{GeV}/c^2)$, which represent the background. The optimal cut value of the BDT has been chosen to maximize the signal yield significance. Tight particle identification (PID) requirements are applied to reduce the combinatorial background and suppress the cross feed between $p\bar{p}K^+$ and $p\bar{p}\pi^+$. The PID efficiencies are derived from calibration data samples of kinematically identified pions, kaons, and protons originating from the decays $D^{*+} \to D^0(\to K^-\pi^+)\pi^+$ and $\Lambda \to p\pi^-$.

Signal and background yields are extracted using unbinned extended maximum likelihood fits to the invariant mass distribution of the $p\bar{p}h^+$ combinations. The $B^+ \to p\bar{p}K^+$ signal is modeled by the sum of two Crystal Ball functions [18], for which the common mean and core width are allowed to float in the fit. Besides the signal component, the fit includes the parametrizations of the combinatorial background and partially reconstructed $B \to p\bar{p}K^*$ decays, where a pion from the K^* decay is not reconstructed, resulting in a $p\bar{p}K$ invariant mass below the nominal B mass. An asymmetric Gaussian function with power-law tails is used to model a possible $p\bar{p}\pi^+$ cross-feed component, where the pion is misidentified as a kaon. This contribution is found to be small.

The fit to the $B^+ \to p\bar{p}\pi^+$ decay uses similar parametrizations for the signal, the combinatorial background, the $p\bar{p}K^+$ cross feed, and the partially reconstructed background from the $B \to p\bar{p}\rho$ decays (with a missing pion from the ρ decay). The cross feed is found to be negligible.

The $B^+ \to p\bar{p}h^+$ invariant mass spectra are shown in Fig. 1. The signal yields obtained from the fits are $N(p\bar{p}K^\pm) = 18721 \pm 142$ and $N(p\bar{p}\pi^\pm) = 1988 \pm 74$, where the uncertainties are statistical only.

The distribution of events in the Dalitz plane—defined by $(m^2_{p\bar{p}}, m^2_{hp})$, where hp denotes the neutral combinations h^-p and $h^+\bar{p}$—is examined. From the fits to the B^+ candidate invariant mass, shown in Fig. 1, signal weights are calculated with the $_s$Plot technique [19]. These weights are corrected for trigger, reconstruction, and selection efficiencies, which are estimated from simulated samples and calibration data. The Dalitz-plot variables are calculated by constraining the $p\bar{p}h^+$ invariant mass to the known B^+ meson mass [20,21]. Figure 2 shows the Dalitz

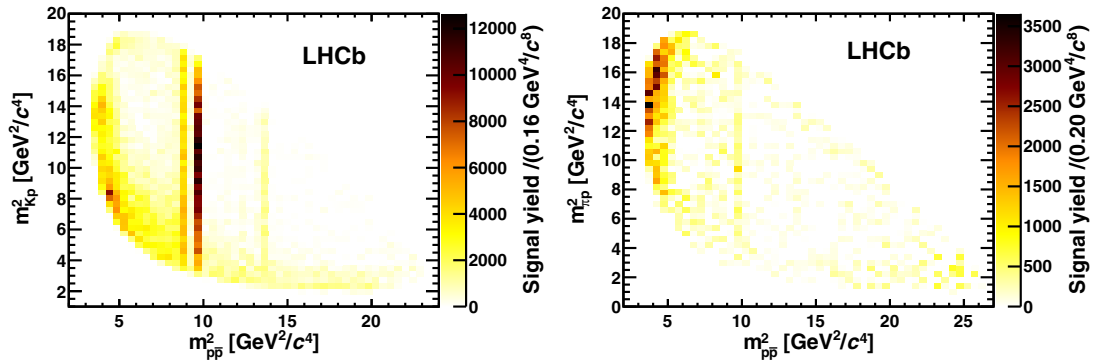

FIG. 2 (color online). Background-subtracted and acceptance-corrected Dalitz-plot distributions for $B^+ \to p\bar{p}K^+$ (left panel) and $B^+ \to p\bar{p}\pi^+$ (right panel).

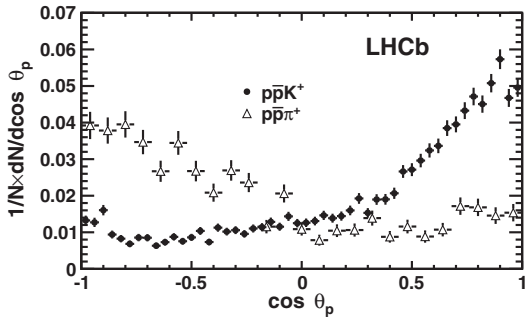

FIG. 3. Background-subtracted and acceptance-corrected normalized distributions of $\cos\theta_p$ for $B^+ \to p\bar{p}K^+$ and $B^+ \to p\bar{p}\pi^+$ decays, for $m_{p\bar{p}} < 2.85$ GeV/c^2. The data points are shown with their total uncertainties.

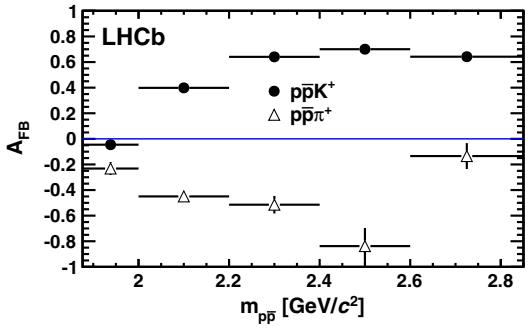

FIG. 4 (color online). Forward-backward asymmetry in bins of $m_{p\bar{p}}$ for $B^+ \to p\bar{p}K^+$ and $B^+ \to p\bar{p}\pi^+$ decays. The data points are shown with their total uncertainties.

distributions of the $B^+ \to p\bar{p}h^+$ events. Similar to the results reported in Refs. [6,22], clear signals of J/ψ, η_c, and $\psi(2S)$ resonances are observed, while $B^+ \to p\bar{p}K^+$ and $B^+ \to p\bar{p}\pi^+$ noncharmonium events both accumulate near the $p\bar{p}$ threshold. However, $B^+ \to p\bar{p}K^+$ events preferentially occupy the region with low Kp invariant mass while $B^+ \to p\bar{p}\pi^+$ events populate the region with large πp invariant mass. This difference in the Dalitz distribution can also be observed as a difference in the distribution of the helicity angle θ_p of the $p\bar{p}$ system, defined as the angle between the charged meson h and the oppositely charged baryon in the rest frame of the $p\bar{p}$ system. The distributions of $\cos(\theta_p)$ are depicted in Fig. 3.

Data and simulation are used to assign systematic uncertainties, accounting for the PID correction and fit model, to the angular and charge asymmetries and to the relative branching fractions. The uncertainty due to the fit model is estimated by considering the impact of varying the fit functions on the yields and raw asymmetries. The systematic uncertainty associated with the PID correction is derived from the combined use of simulation and calibration data samples and cancels in the asymmetry measurements.

The forward-backward (FB) asymmetry is measured as

$$A_{\rm FB} = \frac{N_{\rm pos} - N_{\rm neg}}{N_{\rm pos} + N_{\rm neg}}, \qquad (1)$$

where $N_{\rm pos}$ ($N_{\rm neg}$) is the efficiency-corrected yield for $\cos\theta_p > 0$ ($\cos\theta_p < 0$). The obtained asymmetries are $A_{\rm FB}(p\bar{p}K^+, m_{p\bar{p}} < 2.85\ {\rm GeV}/c^2) = 0.495 \pm 0.012\ ({\rm stat}) \pm 0.007\ ({\rm syst})$ and $A_{\rm FB}(p\bar{p}\pi^+, m_{p\bar{p}} < 2.85\ {\rm GeV}/c^2) = -0.409 \pm 0.033\ ({\rm stat}) \pm 0.006\ ({\rm syst})$, where the systematic uncertainty is due to the ratio of average efficiencies in the regions $\cos\theta_p > 0$ and $\cos\theta_p < 0$. As reported in previous studies [6,23], the value for $B^+ \to p\bar{p}K^+$ contradicts the short-range analysis expectation [24]. The values of $A_{\rm FB}$ in bins of $m_{p\bar{p}}$ are shown in Fig. 4; in both cases, they depend strongly on $m_{p\bar{p}}$.

The yields of the decays $B^+ \to p\bar{p}h^+$ in the region $m_{p\bar{p}} < 2.85$ GeV/c^2 are obtained with the same model used for the integrated signals. Those of the resonant modes are extracted through two-dimensional extended unbinned maximum likelihood fits to invariant mass distributions of $p\bar{p}h^+$ and $p\bar{p}$ or $K^+\bar{p}$, using the same signal and background models for $m_{p\bar{p}}$ or $m_{K^+\bar{p}}$ as in Ref. [6]. The results are shown in Table I. The branching fractions of the decays $B^+ \to \bar{\Lambda}(1520)(\to K^+\bar{p})p$ and $B^+ \to p\bar{p}\pi^+$, $m_{p\bar{p}} < 2.85$ GeV/c^2 are measured relative to the J/ψ modes as

$$\frac{\mathcal{B}(B^+ \to \bar{\Lambda}(1520)(\to K^+\bar{p})p)}{\mathcal{B}(B^+ \to J/\psi(\to p\bar{p})K^+)} = 0.033 \pm 0.005\ ({\rm stat}) \pm 0.007\ ({\rm syst}),$$

$$\frac{\mathcal{B}(B^+ \to p\bar{p}\pi^+, m_{p\bar{p}} < 2.85\ {\rm GeV}/c^2)}{\mathcal{B}(B^+ \to J/\psi(\to p\bar{p})\pi^+)} = 12.0 \pm 1.2\ ({\rm stat}) \pm 0.3\ ({\rm syst}).$$

The systematic uncertainties also include contributions from the background model. Using $\mathcal{B}(B^+ \to J/\psi K^+) = (1.016 \pm 0.033) \times 10^{-3}$, $\mathcal{B}(B^+ \to J/\psi\pi^+) = (4.1 \pm 0.4) \times 10^{-5}$, $\mathcal{B}(J/\psi \to p\bar{p}) = (2.17 \pm 0.07) \times 10^{-3}$ [21], and $\mathcal{B}(\Lambda(1520) \to K^- p) = 0.234 \pm 0.016$ [25], the branching fractions are measured to be $\mathcal{B}(B^+ \to \bar{\Lambda}(1520)p) =$

TABLE I. Event yields and selection efficiency for $B^+ \to p\bar{p}K^+$ and $B^+ \to p\bar{p}\pi^+$ final states.

Mode	Yield	Efficiency (%)
$B^+ \to J/\psi(\to p\bar{p})K^+$	4260 ± 67	1.55 ± 0.02
$B^+ \to \eta_c(\to p\bar{p})K^+$	2182 ± 64	1.47 ± 0.02
$B^+ \to \psi(2S)(\to p\bar{p})K^+$	368 ± 20	1.59 ± 0.02
$B^+ \to \bar{\Lambda}(1520)(\to K^+\bar{p})p$	128 ± 20	1.39 ± 0.01
$B^+ \to p\bar{p}K^+$, $m_{p\bar{p}} < 2.85$ GeV/c^2	8510 ± 104	1.58 ± 0.02
$B^+ \to J/\psi(\to p\bar{p})\pi^+$	122 ± 12	1.07 ± 0.01
$B^+ \to p\bar{p}\pi^+$, $m_{p\bar{p}} < 2.85$ GeV/c^2	1632 ± 64	1.15 ± 0.01

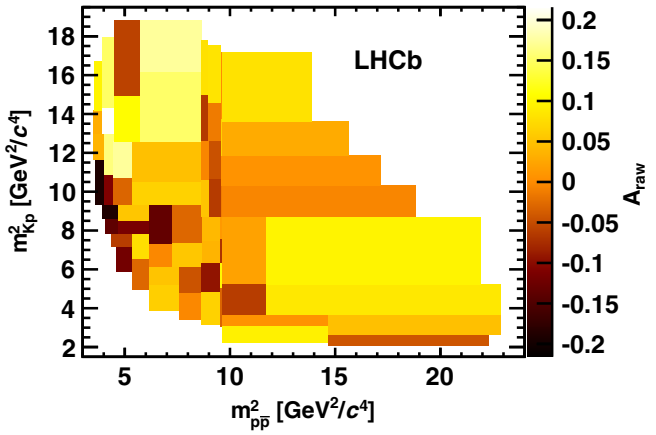

FIG. 5 (color online). Asymmetries of the number of signal events in bins of the Dalitz-plot variables for $B^\pm \to p\bar{p}K^\pm$. The number of events in each bin is approximately 300.

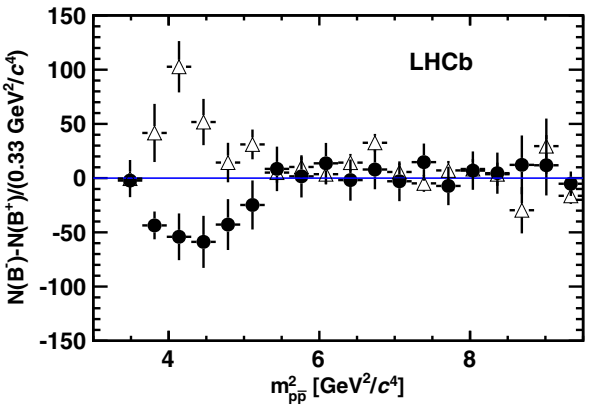

FIG. 6 (color online). $N(B^-) - N(B^+)$ in bins of $m^2_{p\bar{p}}$ for $m^2_{Kp} < 10\ \mathrm{GeV}^2/c^4$ (black filled circles) and $m^2_{Kp} > 10\ \mathrm{GeV}^2/c^4$ (open triangles).

$(3.15 \pm 0.48\ (\mathrm{stat}) \pm 0.07\ (\mathrm{syst}) \pm 0.26\ (\mathrm{BF})) \times 10^{-7}$, $\mathcal{B}(B^+ \to p\bar{p}\pi^+, m_{p\bar{p}} < 2.85\ \mathrm{GeV}/c^2) = (1.07 \pm 0.11\ (\mathrm{stat}) \pm 0.03\ (\mathrm{syst}) \pm 0.11\ (\mathrm{BF})) \times 10^{-6}$, where BF denotes the uncertainty on the aforementioned secondary branching fractions. The former measurement supersedes what is reported in Ref. [6].

The raw charge asymmetry is measured from the yields N as

$$A_{\mathrm{raw}} = \frac{N(B^- \to p\bar{p}h^-) - N(B^+ \to p\bar{p}h^+)}{N(B^- \to p\bar{p}h^-) + N(B^+ \to p\bar{p}h^+)}, \qquad (2)$$

and it is investigated in the Dalitz plane using signal weights inferred from the fits shown in Fig. 1, for B^- and B^+ samples. This asymmetry includes production and detection asymmetries. For the $B^\pm \to p\bar{p}K^\pm$ case, the statistics allows us to perform a full two-dimensional analysis: an adaptative binning algorithm is used so that the sum of B^- and B^+ events in each bin is approximately constant. Figure 5 shows the distribution of A_{raw} in the Dalitz plane. A clear pattern is observed near the $p\bar{p}$ threshold where A_{raw} is negative for $m^2_{Kp} < 10\ \mathrm{GeV}^2/c^4$ and positive for $m^2_{Kp} > 10\ \mathrm{GeV}^2/c^4$. Figure 6 shows the $m^2_{p\bar{p}}$ projections of $N(B^-) - N(B^+)$ in the regions of interest.

To quantify the effect, unbinned extended maximum likelihood simultaneous fits to B^- and B^+ samples are performed in regions of the Dalitz plane, using the same models as the global fits [26]. The raw asymmetry is corrected for acceptance, by taking into account the small difference in average efficiency due to the B^- and B^+ samples populating the Dalitz plane differently. Physical asymmetries are obtained after acceptance correction ($A^{\mathrm{acc}}_{\mathrm{raw}}$) and accounting for the production $A_{\mathrm{P}}(B^\pm)$ and kaon detection $A_{\mathrm{det}}(K^\pm)$ asymmetries:

$$A_{CP} = A^{\mathrm{acc}}_{\mathrm{raw}} - A_{\mathrm{P}}(B^\pm) - A_{\mathrm{det}}(K^\pm). \qquad (3)$$

The decay $B^\pm \to J/\psi(p\bar{p})K^\pm$, part of the selected sample, is used to determine $A_\Delta = A_{\mathrm{P}}(B^\pm) + A_{\mathrm{det}}(K^\pm)$:

$$A_\Delta = A_{\mathrm{raw}}(B^\pm \to J/\psi(p\bar{p})K^\pm) - A_{CP}(B^\pm \to J/\psi K^\pm). \qquad (4)$$

The value $A_{CP}(B^\pm \to J/\psi K^\pm) = (0.6 \pm 0.4)\%$ is taken from Ref. [27]. When using $A_{\mathrm{raw}}(B^\pm \to J/\psi(p\bar{p})K^\pm)$, differences in the momentum asymmetry of the $p\bar{p}$ pair between $B^\pm \to J/\psi(p\bar{p})K^\pm$ and nonresonant $B^\pm \to p\bar{p}K^\pm$ decays are accounted for. A similar procedure

TABLE II. CP asymmetries for $B^\pm \to p\bar{p}K^\pm$ and $B^\pm \to p\bar{p}\pi^\pm$ decays. The systematic uncertainties are dominated by the precision on the measurement $A_{CP}(B^\pm \to J/\psi K^\pm)$.

Mode/region	A_{CP}
$\eta_c(p\bar{p})K^\pm$	$0.040 \pm 0.034\ (\mathrm{stat}) \pm 0.004\ (\mathrm{syst})$
$\psi(2S)(p\bar{p})K^\pm$	$0.092 \pm 0.058\ (\mathrm{stat}) \pm 0.004\ (\mathrm{syst})$
$p\bar{p}K^\pm$, $m_{p\bar{p}} < 2.85\ \mathrm{GeV}/c^2$	$0.021 \pm 0.020\ (\mathrm{stat}) \pm 0.004\ (\mathrm{syst})$
$p\bar{p}K^\pm$, $m_{p\bar{p}} < 2.85\ \mathrm{GeV}/c^2$, $m^2_{Kp} < 10\ \mathrm{GeV}^2/c^4$	$-0.036 \pm 0.023\ (\mathrm{stat}) \pm 0.004\ (\mathrm{syst})$
$p\bar{p}K^\pm$, $m_{p\bar{p}} < 2.85\ \mathrm{GeV}/c^2$, $m^2_{Kp} > 10\ \mathrm{GeV}^2/c^4$	$0.096 \pm 0.024\ (\mathrm{stat}) \pm 0.004\ (\mathrm{syst})$
$p\bar{p}\pi^\pm$, $m_{p\bar{p}} < 2.85\ \mathrm{GeV}/c^2$	$-0.041 \pm 0.039\ (\mathrm{stat}) \pm 0.005\ (\mathrm{syst})$

is applied to obtain $A_{CP}(B^{\pm} \to \eta_c(p\bar{p})K^{\pm})$ and $A_{CP}(B^{\pm} \to \psi(2S)(p\bar{p})K^{\pm})$. The $B^{\pm} \to p\bar{p}\pi^{\pm}$ decays are also considered in the region $m_{p\bar{p}} < 2.85$ GeV/c^2. In this case, the correction also involves the pion detection asymmetry $A'_{\Delta} = A_{\rm raw}(B^{\pm} \to J/\psi(p\bar{p})K^{\pm}) - A_{CP}(B^{\pm} \to J/\psi K^{\pm}) - A_{\rm det}(K^{\pm}) + A_{\rm det}(\pi^{\pm})$. The value $A_{\rm det}(K^{\pm}) - A_{\rm det}(\pi^{\pm}) = (-1.2 \pm 0.1)\%$ is taken from studies of prompt D^+ decays [28]. Table II shows the results, including asymmetries of resonant modes.

The systematic uncertainties are estimated by using alternative fit functions and splitting the data sample according to trigger requirements and magnet polarity. The overall systematic uncertainties are dominated by the uncertainty on the $A_{CP}(B^{\pm} \to J/\psi K^{\pm})$ measurement.

In summary, an interesting sign-inversion pattern of the CP asymmetry appears at low $p\bar{p}$ invariant masses in $B^{\pm} \to p\bar{p}K^{\pm}$ decays. Although this resembles what is observed at low h^+h^- masses in the $B^{\pm} \to h^{\pm}h^+h^-$ decays, the strong phase difference could involve a specific mechanism such as interfering long-range $p\bar{p}$-waves with different angular momenta [24]. In the region $m_{p\bar{p}} < 2.85$ GeV/c^2, $m^2_{Kp} > 10$ GeV^2/c^4, the measured asymmetry is positive with a significance of nearly 4σ, which represents the first evidence of CP violation in b-hadron decays with baryons in the final state. The h-hadron forward-backward asymmetry in noncharmonium $B^+ \to p\bar{p}h^+$ decays is measured as $A_{\rm FB}(p\bar{p}K^+, m_{p\bar{p}} < 2.85\ {\rm GeV}/c^2) = 0.495 \pm 0.012\ ({\rm stat}) \pm 0.007\ ({\rm syst})$ and $A_{\rm FB}(p\bar{p}\pi^+, m_{p\bar{p}} < 2.85\ {\rm GeV}/c^2) = -0.409 \pm 0.033\ ({\rm stat}) \pm 0.006\ ({\rm syst})$. These asymmetries could be interpreted as being due to the dominance of nonresonant $p\bar{p}$ scattering [24]. Finally, an improved measurement of $\mathcal{B}(B^+ \to \bar{\Lambda}(1520)p) = (3.15 \pm 0.48\ ({\rm stat}) \pm 0.07\ ({\rm syst}) \pm 0.26\ ({\rm BF})) \times 10^{-7}$ is obtained.

We express our gratitude to our colleagues in the CERN accelerator departments for the excellent performance of the LHC. We thank the technical and administrative staff at the LHCb institutes. We acknowledge support from CERN and from the national agencies CAPES, CNPq, FAPERJ and FINEP (Brazil); NSFC (China); CNRS/IN2P3 (France); BMBF, DFG, HGF and MPG (Germany); SFI (Ireland); INFN (Italy); FOM and NWO (The Netherlands); MNiSW and NCN (Poland); MEN/IFA (Romania); MinES and FANO (Russia); MinECo (Spain); SNSF and SER (Switzerland); NASU (Ukraine); STFC (United Kingdom); and NSF (U.S.). The Tier1 computing centers are supported by IN2P3 (France), KIT and BMBF (Germany), INFN (Italy), NWO and SURF (The Netherlands), PIC (Spain), and GridPP (United Kingdom). We are indebted to the communities behind the multiple open source software packages on which we depend. We are also thankful for the computing resources and the access to software research and development tools provided by Yandex LLC (Russia). Individual groups or members have received support from EPLANET, Marie Skłodowska-Curie Actions, and ERC (European Union); Conseil général de Haute-Savoie, Labex ENIGMASS, and OCEVU, Région Auvergne (France); RFBR (Russia); XuntaGal and GENCAT (Spain); and the Royal Society and the Royal Commission for the Exhibition of 1851 (United Kingdom).

[1] B. Aubert *et al.* (BABAR Collaboration), Phys. Rev. Lett. **93**, 131801 (2004).
[2] Y. Chao *et al.* (Belle Collaboration), Phys. Rev. Lett. **93**, 191802 (2004).
[3] R. Aaij *et al.* (LHCb Collaboration), Phys. Rev. Lett. **111**, 101801 (2013).
[4] R. Aaij *et al.* (LHCb Collaboration), Phys. Rev. Lett. **112**, 011801 (2014).
[5] R. Aaij *et al.* (LHCb Collaboration), arXiv:1408.5373 [Phys. Rev. D (to be published)].
[6] R. Aaij *et al.* (LHCb Collaboration), Phys. Rev. D **88**, 052015 (2013).
[7] L. Wolfenstein, Phys. Rev. D **43**, 151 (1991).
[8] A. A. Alves, Jr. *et al.* (LHCb Collaboration), JINST **3**, S08005 (2008).
[9] M. Adinolfi *et al.*, Eur. Phys. J. C **73**, 2431 (2013).
[10] T. Sjöstrand, S. Mrenna, and P. Skands, Comput. Phys. Commun. **178**, 852 (2008).
[11] I. Belyaev *et al.*, in *Proceedings of Nuclear Science Symposium Conference Record (NSS/MIC), 2010 IEEE, Knoxville* (IEEE, New York, 2010), p. 1155.
[12] D. J. Lange, Nucl. Instrum. Methods Phys. Res., Sect. A **462**, 152 (2001).
[13] P. Golonka and Z. Was, Eur. Phys. J. C **45**, 97 (2006).
[14] J. Allison *et al.* (GEANT4 Collaboration), IEEE Trans. Nucl. Sci. **53**, 270 (2006); S. Agostinelli *et al.* (GEANT4 Collaboration), Nucl. Instrum. Methods Phys. Res., Sect. A **506**, 250 (2003).
[15] M. Clemencic, G. Corti, S. Easo, C. R. Jones, S. Miglioranzi, M. Pappagallo, and P. Robbe, J. Phys. Conf. Ser. **331**, 032023 (2011).
[16] R. H. Dalitz, Philos. Mag. **44**, 1068 (1953).
[17] L. Breiman, J. H. Friedman, R. A. Olshen, and C. J. Stone, *Classification and Regression Trees* (Chapman and Hall, London, 1984).
[18] T. Skwarnicki, Ph.D. thesis, Institute of Nuclear Physics, 1986.
[19] M. Pivk and F. R. Le Diberder, Nucl. Instrum. Methods Phys. Res., Sect. A **555**, 356 (2005).
[20] W. D. Hulsbergen, Nucl. Instrum. Methods Phys. Res., Sect. A **552**, 566 (2005).
[21] J. Beringer *et al.* (Particle Data Group), Phys. Rev. D **86**, 010001 (2012); K. A. Olive *et al.* (Particle Data Group), Chin. Phys. C **38**, 090001 (2014).
[22] R. Aaij *et al.* (LHCb Collaboration), Eur. Phys. J. C **73**, 2462 (2013).
[23] J.-T. Wei *et al.* (Belle Collaboration), Phys. Lett. B **659**, 80 (2008).
[24] M. Suzuki, J. Phys. G **34**, 283 (2007).
[25] F. W. Wieland *et al.*, Eur. Phys. J. A **47**, 47 (2011); **47**, 133 (E) (2011).

[26] See Supplemental Material at http://link.aps.org/supplemental/10.1103/PhysRevLett.113.141801 for the fits in the range $m_{p\bar{p}} < 2.85$ GeV/c^2, regions $m^2_{Kp} < 10$ GeV$^2/c^4$ and $m^2_{Kp} > 10$ GeV$^2/c^4$.

[27] V. M. Abazov *et al.* (D0 Collaboration), Phys. Rev. Lett. **110**, 241801 (2013).

[28] R. Aaij *et al.* (LHCb Collaboration), J. High Energy Phys. 07 (2014) 041.

R. Aaij,[41] B. Adeva,[37] M. Adinolfi,[46] A. Affolder,[52] Z. Ajaltouni,[5] S. Akar,[6] J. Albrecht,[9] F. Alessio,[38] M. Alexander,[51] S. Ali,[41] G. Alkhazov,[30] P. Alvarez Cartelle,[37] A. A. Alves Jr.,[25,38] S. Amato,[2] S. Amerio,[22] Y. Amhis,[7] L. An,[3] L. Anderlini,[17,a] J. Anderson,[40] R. Andreassen,[57] M. Andreotti,[16,b] J. E. Andrews,[58] R. B. Appleby,[54] O. Aquines Gutierrez,[10] F. Archilli,[38] A. Artamonov,[35] M. Artuso,[59] E. Aslanides,[6] G. Auriemma,[25,c] M. Baalouch,[5] S. Bachmann,[11] J. J. Back,[48] A. Badalov,[36] W. Baldini,[16] R. J. Barlow,[54] C. Barschel,[38] S. Barsuk,[7] W. Barter,[47] V. Batozskaya,[28] V. Battista,[39] A. Bay,[39] L. Beaucourt,[4] J. Beddow,[51] F. Bedeschi,[23] I. Bediaga,[1] S. Belogurov,[31] K. Belous,[35] I. Belyaev,[31] E. Ben-Haim,[8] G. Bencivenni,[18] S. Benson,[38] J. Benton,[46] A. Berezhnoy,[32] R. Bernet,[40] M.-O. Bettler,[47] M. van Beuzekom,[41] A. Bien,[11] S. Bifani,[45] T. Bird,[54] A. Bizzeti,[17,d] P. M. Bjørnstad,[54] T. Blake,[48] F. Blanc,[39] J. Blouw,[10] S. Blusk,[59] V. Bocci,[25] A. Bondar,[34] N. Bondar,[30,38] W. Bonivento,[15,38] S. Borghi,[54] A. Borgia,[59] M. Borsato,[7] T. J. V. Bowcock,[52] E. Bowen,[40] C. Bozzi,[16] T. Brambach,[9] J. van den Brand,[42] J. Bressieux,[39] D. Brett,[54] M. Britsch,[10] T. Britton,[59] J. Brodzicka,[54] N. H. Brook,[46] H. Brown,[52] A. Bursche,[40] G. Busetto,[22,e] J. Buytaert,[38] S. Cadeddu,[15] R. Calabrese,[16,b] M. Calvi,[20,f] M. Calvo Gomez,[36,g] P. Campana,[18,38] D. Campora Perez,[38] A. Carbone,[14,h] G. Carboni,[24,i] R. Cardinale,[19,38,j] A. Cardini,[15] L. Carson,[50] K. Carvalho Akiba,[2] G. Casse,[52] L. Cassina,[20] L. Castillo Garcia,[38] M. Cattaneo,[38] Ch. Cauet,[9] R. Cenci,[58] M. Charles,[8] Ph. Charpentier,[38] M. Chefdeville,[4] S. Chen,[54] S.-F. Cheung,[55] N. Chiapolini,[40] M. Chrzaszcz,[40,26] K. Ciba,[38] X. Cid Vidal,[38] G. Ciezarek,[53] P. E. L. Clarke,[50] M. Clemencic,[38] H. V. Cliff,[47] J. Closier,[38] V. Coco,[38] J. Cogan,[6] E. Cogneras,[5] P. Collins,[38] A. Comerma-Montells,[11] A. Contu,[15] A. Cook,[46] M. Coombes,[46] S. Coquereau,[8] G. Corti,[38] M. Corvo,[16,b] I. Counts,[56] B. Couturier,[38] G. A. Cowan,[50] D. C. Craik,[48] M. Cruz Torres,[60] S. Cunliffe,[53] R. Currie,[50] C. D'Ambrosio,[38] J. Dalseno,[46] P. David,[8] P. N. Y. David,[41] A. Davis,[57] K. De Bruyn,[41] S. De Capua,[54] M. De Cian,[11] J. M. De Miranda,[1] L. De Paula,[2] W. De Silva,[57] P. De Simone,[18] D. Decamp,[4] M. Deckenhoff,[9] L. Del Buono,[8] N. Déléage,[4] D. Derkach,[55] O. Deschamps,[5] F. Dettori,[38] A. Di Canto,[38] H. Dijkstra,[38] S. Donleavy,[52] F. Dordei,[11] M. Dorigo,[39] A. Dosil Suárez,[37] D. Dossett,[48] A. Dovbnya,[43] K. Dreimanis,[52] G. Dujany,[54] F. Dupertuis,[39] P. Durante,[38] R. Dzhelyadin,[35] A. Dziurda,[26] A. Dzyuba,[30] S. Easo,[49,38] U. Egede,[53] V. Egorychev,[31] S. Eidelman,[34] S. Eisenhardt,[50] U. Eitschberger,[9] R. Ekelhof,[9] L. Eklund,[51] I. El Rifai,[5] Ch. Elsasser,[40] S. Ely,[59] S. Esen,[11] H.-M. Evans,[47] T. Evans,[55] A. Falabella,[14] C. Färber,[11] C. Farinelli,[41] N. Farley,[45] S. Farry,[52] RF Fay,[52] D. Ferguson,[50] V. Fernandez Albor,[37] F. Ferreira Rodrigues,[1] M. Ferro-Luzzi,[38] S. Filippov,[33] M. Fiore,[16,b] M. Fiorini,[16,b] M. Firlej,[27] C. Fitzpatrick,[39] T. Fiutowski,[27] M. Fontana,[10] F. Fontanelli,[19,j] R. Forty,[38] O. Francisco,[2] M. Frank,[38] C. Frei,[38] M. Frosini,[17,38,a] J. Fu,[21,38] E. Furfaro,[24,i] A. Gallas Torreira,[37] D. Galli,[14,h] S. Gallorini,[22] S. Gambetta,[19,j] M. Gandelman,[2] P. Gandini,[59] Y. Gao,[3] J. García Pardiñas,[37] J. Garofoli,[59] J. Garra Tico,[47] L. Garrido,[36] C. Gaspar,[38] R. Gauld,[55] L. Gavardi,[9] G. Gavrilov,[30] E. Gersabeck,[11] M. Gersabeck,[54] T. Gershon,[48] Ph. Ghez,[4] A. Gianelle,[22] S. Giani',[39] V. Gibson,[47] L. Giubega,[29] V. V. Gligorov,[38] C. Göbel,[60] D. Golubkov,[31] A. Golutvin,[53,31,38] A. Gomes,[1,k] C. Gotti,[20] M. Grabalosa Gándara,[5] R. Graciani Diaz,[36] L. A. Granado Cardoso,[38] E. Graugés,[36] G. Graziani,[17] A. Grecu,[29] E. Greening,[55] S. Gregson,[47] P. Griffith,[45] L. Grillo,[11] O. Grünberg,[62] B. Gui,[59] E. Gushchin,[33] Yu. Guz,[35,38] T. Gys,[38] C. Hadjivasiliou,[59] G. Haefeli,[39] C. Haen,[38] S. C. Haines,[47] S. Hall,[53] B. Hamilton,[58] T. Hampson,[46] X. Han,[11] S. Hansmann-Menzemer,[11] N. Harnew,[55] S. T. Harnew,[46] J. Harrison,[54] J. He,[38] T. Head,[38] V. Heijne,[41] K. Hennessy,[52] P. Henrard,[5] L. Henry,[8] J. A. Hernando Morata,[37] E. van Herwijnen,[38] M. Heß,[62] A. Hicheur,[1] D. Hill,[55] M. Hoballah,[5] C. Hombach,[54] W. Hulsbergen,[41] P. Hunt,[55] N. Hussain,[55] D. Hutchcroft,[52] D. Hynds,[51] M. Idzik,[27] P. Ilten,[56] R. Jacobsson,[38] A. Jaeger,[11] J. Jalocha,[55] E. Jans,[41] P. Jaton,[39] A. Jawahery,[58] F. Jing,[3] M. John,[55] D. Johnson,[55] C. R. Jones,[47] C. Joram,[38] B. Jost,[38] N. Jurik,[59] M. Kaballo,[9] S. Kandybei,[43] W. Kanso,[6] M. Karacson,[38] T. M. Karbach,[38] S. Karodia,[51] M. Kelsey,[59] I. R. Kenyon,[45] T. Ketel,[42] B. Khanji,[20] C. Khurewathanakul,[39] S. Klaver,[54] K. Klimaszewski,[28] O. Kochebina,[7] M. Kolpin,[11] I. Komarov,[39] R. F. Koopman,[42] P. Koppenburg,[41,38] M. Korolev,[32] A. Kozlinskiy,[41] L. Kravchuk,[33] K. Kreplin,[11] M. Kreps,[48] G. Krocker,[11] P. Krokovny,[34] F. Kruse,[9] W. Kucewicz,[26,l] M. Kucharczyk,[20,26,38,f] V. Kudryavtsev,[34] K. Kurek,[28] T. Kvaratskheliya,[31] V. N. La Thi,[39] D. Lacarrere,[38] G. Lafferty,[54] A. Lai,[15] D. Lambert,[50]

R. W. Lambert,[42] G. Lanfranchi,[18] C. Langenbruch,[48] B. Langhans,[38] T. Latham,[48] C. Lazzeroni,[45] R. Le Gac,[6] J. van Leerdam,[41] J.-P. Lees,[4] R. Lefèvre,[5] A. Leflat,[32] J. Lefrançois,[7] S. Leo,[23] O. Leroy,[6] T. Lesiak,[26] B. Leverington,[11] Y. Li,[3] T. Likhomanenko,[63] M. Liles,[52] R. Lindner,[38] C. Linn,[38] F. Lionetto,[40] B. Liu,[15] S. Lohn,[38] I. Longstaff,[51] J. H. Lopes,[2] N. Lopez-March,[39] P. Lowdon,[40] H. Lu,[3] D. Lucchesi,[22,e] H. Luo,[50] A. Lupato,[22] E. Luppi,[16,b] O. Lupton,[55] F. Machefert,[7] I. V. Machikhiliyan,[31] F. Maciuc,[29] O. Maev,[30] S. Malde,[55] A. Malinin,[63] G. Manca,[15,m] G. Mancinelli,[6] J. Maratas,[5] J. F. Marchand,[4] U. Marconi,[14] C. Marin Benito,[36] P. Marino,[23,n] R. Märki,[39] J. Marks,[11] G. Martellotti,[25] A. Martens,[8] A. Martín Sánchez,[7] M. Martinelli,[41] D. Martinez Santos,[42] F. Martinez Vidal,[64] D. Martins Tostes,[2] A. Massafferri,[1] R. Matev,[38] Z. Mathe,[38] C. Matteuzzi,[20] A. Mazurov,[16,b] M. McCann,[53] J. McCarthy,[45] A. McNab,[54] R. McNulty,[12] B. McSkelly,[52] B. Meadows,[57] F. Meier,[9] M. Meissner,[11] M. Merk,[41] D. A. Milanes,[8] M.-N. Minard,[4] N. Moggi,[14] J. Molina Rodriguez,[60] S. Monteil,[5] M. Morandin,[22] P. Morawski,[27] A. Mordà,[6] M. J. Morello,[23,n] J. Moron,[27] A.-B. Morris,[50] R. Mountain,[59] F. Muheim,[50] K. Müller,[40] M. Mussini,[14] B. Muster,[39] P. Naik,[46] T. Nakada,[39] R. Nandakumar,[49] I. Nasteva,[2] M. Needham,[50] N. Neri,[21] S. Neubert,[38] N. Neufeld,[38] M. Neuner,[11] A. D. Nguyen,[39] T. D. Nguyen,[39] C. Nguyen-Mau,[39,o] M. Nicol,[7] V. Niess,[5] R. Niet,[9] N. Nikitin,[32] T. Nikodem,[11] A. Novoselov,[35] D. P. O'Hanlon,[48] A. Oblakowska-Mucha,[27] V. Obraztsov,[35] S. Oggero,[41] S. Ogilvy,[51] O. Okhrimenko,[44] R. Oldeman,[15,m] G. Onderwater,[65] M. Orlandea,[29] J. M. Otalora Goicochea,[2] P. Owen,[53] A. Oyanguren,[64] B. K. Pal,[59] A. Palano,[13,p] F. Palombo,[21,q] M. Palutan,[18] J. Panman,[38] A. Papanestis,[49,38] M. Pappagallo,[51] L. L. Pappalardo,[16,b] C. Parkes,[54] C. J. Parkinson,[9,45] G. Passaleva,[17] G. D. Patel,[52] M. Patel,[53] C. Patrignani,[19,j] A. Pazos Alvarez,[37] A. Pearce,[54] A. Pellegrino,[41] M. Pepe Altarelli,[38] S. Perazzini,[14,h] E. Perez Trigo,[37] P. Perret,[5] M. Perrin-Terrin,[6] L. Pescatore,[45] E. Pesen,[66] K. Petridis,[53] A. Petrolini,[19,j] E. Picatoste Olloqui,[36] B. Pietrzyk,[4] T. Pilař,[48] D. Pinci,[25] A. Pistone,[19] S. Playfer,[50] M. Plo Casasus,[37] F. Polci,[8] A. Poluektov,[48,34] E. Polycarpo,[2] A. Popov,[35] D. Popov,[10] B. Popovici,[29] C. Potterat,[2] E. Price,[46] J. Prisciandaro,[39] A. Pritchard,[52] C. Prouve,[46] V. Pugatch,[44] A. Puig Navarro,[39] G. Punzi,[23,r] W. Qian,[4] B. Rachwal,[26] J. H. Rademacker,[46] B. Rakotomiaramanana,[39] M. Rama,[18] M. S. Rangel,[2] I. Raniuk,[43] N. Rauschmayr,[38] G. Raven,[42] S. Reichert,[54] M. M. Reid,[48] A. C. dos Reis,[1] S. Ricciardi,[49] S. Richards,[46] M. Rihl,[38] K. Rinnert,[52] V. Rives Molina,[36] D. A. Roa Romero,[5] P. Robbe,[7] A. B. Rodrigues,[1] E. Rodrigues,[54] P. Rodriguez Perez,[54] S. Roiser,[38] V. Romanovsky,[35] A. Romero Vidal,[37] M. Rotondo,[22] J. Rouvinet,[39] T. Ruf,[38] F. Ruffini,[23] H. Ruiz,[36] P. Ruiz Valls,[64] J. J. Saborido Silva,[37] N. Sagidova,[30] P. Sail,[51] B. Saitta,[15,m] V. Salustino Guimaraes,[2] C. Sanchez Mayordomo,[64] B. Sanmartin Sedes,[37] R. Santacesaria,[25] C. Santamarina Rios,[37] E. Santovetti,[24,i] A. Sarti,[18,s] C. Satriano,[25,c] A. Satta,[24] D. M. Saunders,[46] M. Savrie,[16,b] D. Savrina,[31,32] M. Schiller,[42] H. Schindler,[38] M. Schlupp,[9] M. Schmelling,[10] B. Schmidt,[38] O. Schneider,[39] A. Schopper,[38] M.-H. Schune,[7] R. Schwemmer,[38] B. Sciascia,[18] A. Sciubba,[25] M. Seco,[37] A. Semennikov,[31] I. Sepp,[53] N. Serra,[40] J. Serrano,[6] L. Sestini,[22] P. Seyfert,[11] M. Shapkin,[35] I. Shapoval,[16,43,b] Y. Shcheglov,[30] T. Shears,[52] L. Shekhtman,[34] V. Shevchenko,[63] A. Shires,[9] R. Silva Coutinho,[48] G. Simi,[22] M. Sirendi,[47] N. Skidmore,[46] T. Skwarnicki,[59] N. A. Smith,[52] E. Smith,[55,49] E. Smith,[53] J. Smith,[47] M. Smith,[54] H. Snoek,[41] M. D. Sokoloff,[57] F. J. P. Soler,[51] F. Soomro,[39] D. Souza,[46] B. Souza De Paula,[2] B. Spaan,[9] A. Sparkes,[50] P. Spradlin,[51] S. Sridharan,[38] F. Stagni,[38] M. Stahl,[11] S. Stahl,[11] O. Steinkamp,[40] O. Stenyakin,[35] S. Stevenson,[55] S. Stoica,[29] S. Stone,[59] B. Storaci,[40] S. Stracka,[23,38] M. Straticiuc,[29] U. Straumann,[40] R. Stroili,[22] V. K. Subbiah,[38] L. Sun,[57] W. Sutcliffe,[53] K. Swientek,[27] S. Swientek,[9] V. Syropoulos,[42] M. Szczekowski,[28] P. Szczypka,[39,38] D. Szilard,[2] T. Szumlak,[27] S. T'Jampens,[4] M. Teklishyn,[7] G. Tellarini,[16,b] F. Teubert,[38] C. Thomas,[55] E. Thomas,[38] J. van Tilburg,[41] V. Tisserand,[4] M. Tobin,[39] S. Tolk,[42] L. Tomassetti,[16,b] D. Tonelli,[38] S. Topp-Joergensen,[55] N. Torr,[55] E. Tournefier,[4] S. Tourneur,[39] M. T. Tran,[39] M. Tresch,[40] A. Tsaregorodtsev,[6] P. Tsopelas,[41] N. Tuning,[41] M. Ubeda Garcia,[38] A. Ukleja,[28] A. Ustyuzhanin,[63] U. Uwer,[11] V. Vagnoni,[14] G. Valenti,[14] A. Vallier,[7] R. Vazquez Gomez,[18] P. Vazquez Regueiro,[37] C. Vázquez Sierra,[37] S. Vecchi,[16] J. J. Velthuis,[46] M. Veltri,[17,t] G. Veneziano,[39] M. Vesterinen,[11] B. Viaud,[7] D. Vieira,[2] M. Vieites Diaz,[37] X. Vilasis-Cardona,[36,g] A. Vollhardt,[40] D. Volyanskyy,[10] D. Voong,[46] A. Vorobyev,[30] V. Vorobyev,[34] C. Voß,[62] H. Voss,[10] J. A. de Vries,[41] R. Waldi,[62] C. Wallace,[48] R. Wallace,[12] J. Walsh,[23] S. Wandernoth,[11] J. Wang,[59] D. R. Ward,[47] N. K. Watson,[45] D. Websdale,[53] M. Whitehead,[48] J. Wicht,[38] D. Wiedner,[11] G. Wilkinson,[55] M. P. Williams,[45] M. Williams,[56] F. F. Wilson,[49] J. Wimberley,[58] J. Wishahi,[9] W. Wislicki,[28] M. Witek,[26] G. Wormser,[7] S. A. Wotton,[47] S. Wright,[47] S. Wu,[3] K. Wyllie,[38] Y. Xie,[61] Z. Xing,[59] Z. Xu,[39] Z. Yang,[3] X. Yuan,[3] O. Yushchenko,[35] M. Zangoli,[14] M. Zavertyaev,[10,u] L. Zhang,[59] W. C. Zhang,[12] Y. Zhang,[3] A. Zhelezov,[11] A. Zhokhov,[31] L. Zhong[3] and A. Zvyagin[38]

(LHCb Collaboration)

[1]Centro Brasileiro de Pesquisas Físicas (CBPF), Rio de Janeiro, Brazil
[2]Universidade Federal do Rio de Janeiro (UFRJ), Rio de Janeiro, Brazil
[3]Center for High Energy Physics, Tsinghua University, Beijing, China
[4]LAPP, Université de Savoie, CNRS/IN2P3, Annecy-Le-Vieux, France
[5]Clermont Université, Université Blaise Pascal, CNRS/IN2P3, LPC, Clermont-Ferrand, France
[6]CPPM, Aix-Marseille Université, CNRS/IN2P3, Marseille, France
[7]LAL, Université Paris-Sud, CNRS/IN2P3, Orsay, France
[8]LPNHE, Université Pierre et Marie Curie, Université Paris Diderot, CNRS/IN2P3, Paris, France
[9]Fakultät Physik, Technische Universität Dortmund, Dortmund, Germany
[10]Max-Planck-Institut für Kernphysik (MPIK), Heidelberg, Germany
[11]Physikalisches Institut, Ruprecht-Karls-Universität Heidelberg, Heidelberg, Germany
[12]School of Physics, University College Dublin, Dublin, Ireland
[13]Sezione INFN di Bari, Bari, Italy
[14]Sezione INFN di Bologna, Bologna, Italy
[15]Sezione INFN di Cagliari, Cagliari, Italy
[16]Sezione INFN di Ferrara, Ferrara, Italy
[17]Sezione INFN di Firenze, Firenze, Italy
[18]Laboratori Nazionali dell'INFN di Frascati, Frascati, Italy
[19]Sezione INFN di Genova, Genova, Italy
[20]Sezione INFN di Milano Bicocca, Milano, Italy
[21]Sezione INFN di Milano, Milano, Italy
[22]Sezione INFN di Padova, Padova, Italy
[23]Sezione INFN di Pisa, Pisa, Italy
[24]Sezione INFN di Roma Tor Vergata, Roma, Italy
[25]Sezione INFN di Roma La Sapienza, Roma, Italy
[26]Henryk Niewodniczanski Institute of Nuclear Physics Polish Academy of Sciences, Kraków, Poland
[27]AGH-University of Science and Technology, Faculty of Physics and Applied Computer Science, Kraków, Poland
[28]National Center for Nuclear Research (NCBJ), Warsaw, Poland
[29]Horia Hulubei National Institute of Physics and Nuclear Engineering, Bucharest-Magurele, Romania
[30]Petersburg Nuclear Physics Institute (PNPI), Gatchina, Russia
[31]Institute of Theoretical and Experimental Physics (ITEP), Moscow, Russia
[32]Institute of Nuclear Physics, Moscow State University (SINP MSU), Moscow, Russia
[33]Institute for Nuclear Research of the Russian Academy of Sciences (INR RAN), Moscow, Russia
[34]Budker Institute of Nuclear Physics (SB RAS) and Novosibirsk State University, Novosibirsk, Russia
[35]Institute for High Energy Physics (IHEP), Protvino, Russia
[36]Universitat de Barcelona, Barcelona, Spain
[37]Universidad de Santiago de Compostela, Santiago de Compostela, Spain
[38]European Organization for Nuclear Research (CERN), Geneva, Switzerland
[39]Ecole Polytechnique Fédérale de Lausanne (EPFL), Lausanne, Switzerland
[40]Physik-Institut, Universität Zürich, Zürich, Switzerland
[41]Nikhef National Institute for Subatomic Physics, Amsterdam, The Netherlands
[42]Nikhef National Institute for Subatomic Physics and VU University Amsterdam, Amsterdam, The Netherlands
[43]NSC Kharkiv Institute of Physics and Technology (NSC KIPT), Kharkiv, Ukraine
[44]Institute for Nuclear Research of the National Academy of Sciences (KINR), Kyiv, Ukraine
[45]University of Birmingham, Birmingham, United Kingdom
[46]H.H. Wills Physics Laboratory, University of Bristol, Bristol, United Kingdom
[47]Cavendish Laboratory, University of Cambridge, Cambridge, United Kingdom
[48]Department of Physics, University of Warwick, Coventry, United Kingdom
[49]STFC Rutherford Appleton Laboratory, Didcot, United Kingdom
[50]School of Physics and Astronomy, University of Edinburgh, Edinburgh, United Kingdom
[51]School of Physics and Astronomy, University of Glasgow, Glasgow, United Kingdom
[52]Oliver Lodge Laboratory, University of Liverpool, Liverpool, United Kingdom
[53]Imperial College London, London, United Kingdom
[54]School of Physics and Astronomy, University of Manchester, Manchester, United Kingdom
[55]Department of Physics, University of Oxford, Oxford, United Kingdom
[56]Massachusetts Institute of Technology, Cambridge, Massachusetts 02139, USA
[57]University of Cincinnati, Cincinnati, Ohio 45221, USA
[58]University of Maryland, College Park, Maryland 20742, USA
[59]Syracuse University, Syracuse, New York, USA

[60]*Pontifícia Universidade Católica do Rio de Janeiro (PUC-Rio), Rio de Janeiro, Brazil (associated with Institution Universidade Federal do Rio de Janeiro (UFRJ), Rio de Janeiro, Brazil)*
[61]*Institute of Particle Physics, Central China Normal University, Wuhan, Hubei, China (associated with Institution Center for High Energy Physics, Tsinghua University, Beijing, China)*
[62]*Institut für Physik, Universität Rostock, Rostock, Germany (associated with Institution Physikalisches Institut, Ruprecht-Karls-Universität Heidelberg, Heidelberg, Germany)*
[63]*National Research Centre Kurchatov Institute, Moscow, Russia (associated with Institution Institute of Theoretical and Experimental Physics (ITEP), Moscow, Russia)*
[64]*Instituto de Fisica Corpuscular (IFIC), Universitat de Valencia-CSIC, Valencia, Spain (associated with Institution Universitat de Barcelona, Barcelona, Spain)*
[65]*KVI-University of Groningen, Groningen, The Netherlands (associated with Institution Nikhef National Institute for Subatomic Physics, Amsterdam, The Netherlands)*
[66]*Celal Bayar University, Manisa, Turkey (associated with Institution European Organization for Nuclear Research (CERN), Geneva, Switzerland)*

[a]Also at Università di Firenze, Firenze, Italy.
[b]Also at Università di Ferrara, Ferrara, Italy.
[c]Also at Università della Basilicata, Potenza, Italy.
[d]Also at Università di Modena e Reggio Emilia, Modena, Italy.
[e]Also at Università di Padova, Padova, Italy.
[f]Also at Università di Milano Bicocca, Milano, Italy.
[g]Also at LIFAELS, La Salle, Universitat Ramon Llull, Barcelona, Spain.
[h]Also at Università di Bologna, Bologna, Italy.
[i]Also at Università di Roma Tor Vergata, Roma, Italy.
[j]Also at Università di Genova, Genova, Italy.
[k]Also at Universidade Federal do Triângulo Mineiro (UFTM), Uberaba-MG, Brazil.
[l]Also at AGH - University of Science and Technology, Faculty of Computer Science, Electronics and Telecommunications, Kraków, Poland.
[m]Also at Università di Cagliari, Cagliari, Italy.
[n]Also at Scuola Normale Superiore, Pisa, Italy.
[o]Also at Hanoi University of Science, Hanoi, Vietnam.
[p]Also at Università di Bari, Bari, Italy.
[q]Also at Università degli Studi di Milano, Milano, Italy.
[r]Also at Università di Pisa, Pisa, Italy.
[s]Also at Università di Roma La Sapienza, Roma, Italy.
[t]Also at Università di Urbino, Urbino, Italy.
[u]Also at P.N. Lebedev Physical Institute, Russian Academy of Science (LPI RAS), Moscow, Russia.